VOLUME 12 NOMOR 1 JUNE 2025 ISSN 2548 – 611X

JURNAL
BIOTEKNOLOGI & BIOSAINS INDONESIA

Homepage Jurnal: http://ejournal.brin.go.id/JBBI/index

IDENTIFICATION OF KEY NITROGEN USE EFFICIENCY-RELATED GENES IN OIL PALM USING BIOINFORMATICS APPROACHES

Identifikasi Gen Kunci terkait Efisiensi Penggunaan Nitrogen pada Kelapa Sawit Menggunakan Pendekatan Bioinformatika

Galuh Wening Permatasari[1], Retno Diah Setiowati[1], Sri Wening[1]*
[1]Indonesian Oil Palm Research Institute (IOPRI) – PT Riset Perkebunan Nusantara,
Brigjend Katamso St. No. 51, Medan, North Sumatera
*Email: sriwening.sw@gmail.com

ABSTRACT
Efficient nitrogen use is crucial for maximizing oil palm yield while reducing environmental impact. Poor nitrogen utilization causes excessive growth and nutrient loss. This study uses bioinformatics to identify key genes linked to nitrogen use efficiency, providing insights for genetic improvement and sustainable cultivation.Protein-protein interaction (PPI) networks, functional enrichment, and structural modeling were employed to uncover candidate genes regulating nitrogen uptake and metabolism. Sixty-two nitrogen use efficiency associated genes from rice (*Oryza sativa*) were analyzed via BLASTp against the *E. guineensis* genome (NCBI), selecting those with >80% similarity. PPI networks were constructed using STRING-db and analyzed in Cytoscape v3.7.1. Functional enrichment (Gene Ontology) and structural analysis (AlphaFold, PyMol v2.5.4) were performed. Twelve nitrogen use efficiency related genes were identified, with CESA4, CESA7, and CESA9 emerging as key regulators based on high degree and betweenness values in PPI analysis. These genes are linked to plant cell wall biosynthesis. Structural analysis showed high similarity to rice homologs, with RMSD values of 0.338 Å (CESA4) and 0.396 Å (CESA9), indicating strong conservation area. Their structural relevance suggests they are promising targets for molecular breeding marker to enhance nitrogen utilization and sustainability in oil palm.

Keywords: *Nitrogen use efficiency, Protein-protein interaction, Structural modeling, CESA genes*

ABSTRAK
Penggunaan nitrogen yang efisien penting untuk meningkatkan hasil kelapa sawit dan mengurangi dampak lingkungan. Studi ini menggunakan bioinformatika untuk mengidentifikasi gen kunci terkait efisiensi nitrogen guna perbaikan genetik dan budidaya berkelanjutan. Interaksi protein-protein (PPI), analisis pengayaan fungsional, dan pemodelan struktural digunakan untuk mengungkap gen kandidat yang mengatur penyerapan dan metabolisme nitrogen. Sebanyak 62 gen dari padi dianalisis dengan BLASTp terhadap genom *E. guineensis* (NCBI) dan diseleksi berdasarkan kesamaan >80%. Jaringan interaksi protein-protein (PPI) dikonstruksi menggunakan STRING-db dan dianalisis di Cytoscape v3.7.1, sementara analisis pengayaan fungsional (Gene Ontology) serta analisis struktural (AlphaFold, PyMol v2.5.4) dilakukan. Sebanyak 12 gen terkait efisiensi nitrogen diidentifikasi, dengan CESA4, CESA7, dan CESA9 sebagai regulator utama dalam analisis PPI. Gen-gen ini berperan dalam biosintesis dinding sel tanaman. Kesamaan struktural tinggi dengan homolog padi (RMSD 0,338–0,396 Å) menunjukkan konservasi yang kuat, menjadikannya target potensial untuk penanda molekuler guna meningkatkan efisiensi nitrogen dan keberlanjutan kelapa sawit.

Received: *15 March 2025* ***Accepted***: *28 April 2025* ***Published***: *18 June 2025*

Kata kunci: *Efisiensi penggunaan nitrogen, interaksi protein-protein, pemodelan struktural, gen CESA*

.

INTRODUCTION

Nitrogen use efficiency is crucial for oil palm cultivation as it directly affects yield, cost-effectiveness, and environmental sustainability. Nitrogen is a key nutrient required for frond development, vegetative growth, and fresh fruit bunch (FFB) production which determines oil yield (Corley and Tinker 2016). However, inefficient nitrogen use can lead to excessive vegetative growth at the expense of fruit production, reducing overall profitability. Additionally, nitrogen losses through leaching, volatilization, and denitrification contribute to environmental issues, such as groundwater contamination and greenhouse gas emissions (Wei et al. 2024).

Nitrous oxide (N_2O) emissions from nitrogen fertilizer application during different growth stages of oil palm were assessed across plantations of varying palm ages. The released N_2O ranged from 19.11 to 22.17 kg N_2O-N per hectare, contributing to carbon dioxide equivalent (CO_2-eq) emissions between 1052.26 and 1209.51 kg per hectare (Kusin et al. 2015). This highlights the need for improved nitrogen management strategies to balance productivity and environmental impact. Selecting oil palm genotypes with higher nitrogen uptake efficiency and optimizing fertilizer application methods can significantly enhance nitrogen use efficiency. To produce planting materials with high nutrient use efficiency, a plant breeding program is needed to develop nutrient-efficient planting materials. However, conventional oil palm breeding programs face challenges due to the long life cycle of oil palm, resulting in lengthy selection cycles. This issue can be addressed by utilizing molecular markers to assist in the selection process (Lema, 2018).

Molecular markers associated with nitrogen use efficiency traits have emerged as valuable tools in breeding programs to develop oil palm varieties with improved nitrogen uptake and assimilation capabilities. Research has demonstrated that oil palm genotypes exhibit differential responses to nitrogen sources, such as ammonium and nitrate, under varying environmental conditions. A study assessing the interaction between nitrogen source and drought stress in oil palm seedlings found significant genotypic variability in traits related to nitrogen metabolism and stress tolerance. This suggests that integrating molecular markers associated with nitrogen source preference and stress resilience can aid in selecting genotypes with optimized nitrogen use efficiency under specific environmental conditions (Ruiz-Romero et al. 2024). Additionally, the development of molecular markers linked to genes involved in nitrogen metabolism, such as purple acid phosphatases, has shown promise in distinguishing between high and low-nitrogen-efficient oil palm progenies. These markers facilitate the early selection of desirable traits, accelerating the breeding process and improving nitrogen use efficiency (Maryanto et al. 2021).

To achieve sustainable agriculture, it is essential to enhance the efficiency of nitrogen utilization in oil palm (*Elaeis guineensis*). However, conventional breeding approaches are hindered by the crop's long-life cycle, resulting in prolonged selection processes. The integration of molecular markers through protein-protein interaction (PPI) bioinformatics presents a promising strategy for accelerating precision-driven selection. This approach has the potential to significantly improve nitrogen use efficiency in oil palm, thereby advancing breeding programs and contributing to more sustainable agricultural practices. PPI networks are able to identify key proteins involved in nitrogen metabolism, enabling the discovery of candidate genes associated with nitrogen use efficiency. For instance, research has demonstrated that heterotrimeric G proteins significantly influence nitrogen use efficiency in rice (*Oryza sativa*), suggesting that similar regulatory mechanisms may exist in oil palm (Sun et al. 2014). By constructing PPI networks, researchers can pinpoint hub proteins that regulate nitrogen uptake and assimilation, facilitating the development of molecular markers for breeding programs.

Proteomics technologies have been applied in oil palm research to understand protein expression changes related to various traits (Lau et al. 2018). Integrating PPI bioinformatics with proteomics data can enhance the identification of nitrogen use efficiency-related markers, leading to the development of oil palm cultivars with improved nitrogen utilization. This approach not only boosts crop productivity but also reduces environmental impacts associated with excessive nitrogen fertilization. Therefore, employing PPI bioinformatics in marker development is a strategic advancement toward sustainable oil palm cultivation.

MATERIALS AND METHODS

The steps for screening and selecting important genes for nutrient use efficiency in oil palm are illustrated in Figure 1.

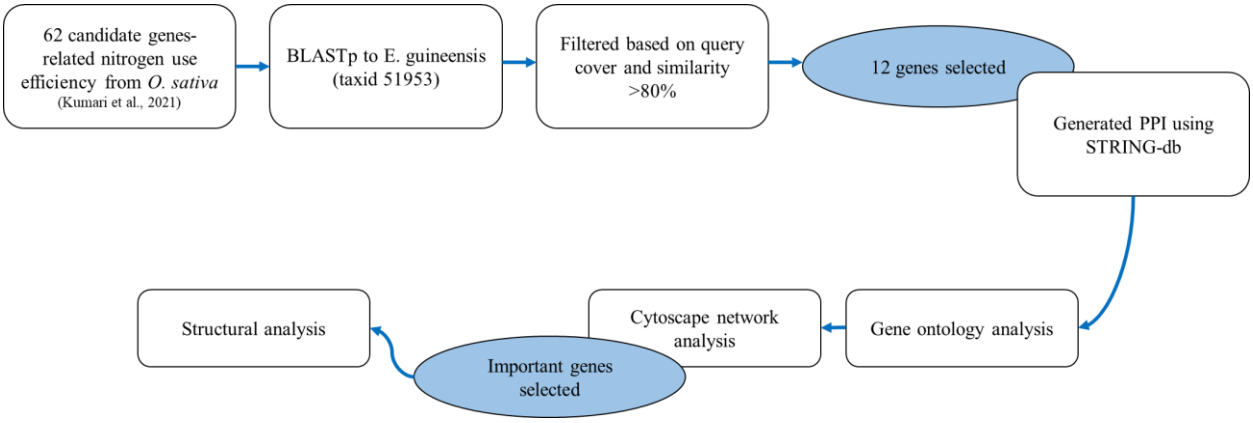

Figure 1. Screening workflow for identifying candidate genes associated with nitrogen use efficiency in *E. guineensis*

Screening methods

A total of 62 genes associated with nitrogen use efficiency in *Oryza sativa* were identified in a study by Kumari et al. (2021). These genes served as the initial pool of candidates for selecting potential regulators of nitrogen use efficiency in *Elaeis guineensis*. The 62 genes were subsequently subjected to a BLASTp (blast.ncbi.nlm.nih.gov/Blast.cgi) search against the NCBI database, with the search restricted to the *E. guineensis* organism (taxid:51953). The results were then filtered to include only those genes exhibiting more than 80% sequence similarity and query coverage, ensuring a high degree of sequence resemblance.

Protein-protein interaction (PPI) analysis

The STRING database (string-db.org) was employed to construct the protein-protein interaction (PPI) network, and Cytoscape v3.7.1 software (cytoscape.org) was subsequently used to visualize the network, with edge betweenness and degree as key parameters. The degree was utilized to represent the node size, while betweenness determined the edge thickness. Cytoscape, an open-source software, is widely used to visualize and analyze complex biological networks, such as metabolic pathways, gene regulatory networks, and protein-protein interactions. Its popularity in systems biology and bioinformatics stems from its ability to integrate network data with annotations, functional enrichment, and other advanced analytical techniques (Doncheva et al. 2023).

Functional enrichment analysis

Gene ontology data, including biological processes, molecular functions, cellular components, subcellular locations, and KEGG pathways, were automatically retrieved from the STRING database (string-db.org). Functional enrichment was visualized by grouping terms with a similarity score of ≥0.8. STRING (Search Tool for the Retrieval of Interacting Genes/Proteins) is a comprehensive database that provides in-

formation on both known and predicted protein-protein interactions (PPIs). It integrates data from multiple sources, including text mining, computational predictions, and experimental findings, to build extensive interaction networks across different organisms (Szklarczyk et al. 2021).

Structural analysis

To ensure structural similarities between *Oryza sativa* and *Elaeis guineensis*, we analyzed the 3D protein structures of selected genes. AlphaFold (alphafold.ebi.ac.uk/), a deep learning-based software, was employed to predict the 3D structures. AlphaFold, evaluated during the CASP14 assessment (May–July 2020) under the name "AlphaFold2," utilizes an advanced model distinct from its CASP13 version. The Critical Assessment of Structure Prediction (CASP) is held biennially and uses recently solved but unpublished protein structures for blind tests to evaluate prediction accuracy (Jumper et al. 2021). The quality of the 3D structures generated by Alphafold was then evaluated using a Ramachandran plot, utilizing Ramplot tools (ramplot.in/index.php). The PyMOL Molecular Graphics System v.2.5.4 (Schrödinger, LLC) was then used to superimpose the structures.

RESULTS AND DISCUSSION

Global alignment to *E. guineensis* taxid

In this study, we utilized the meta-analysis results from Kumari et al. (2021) as the basis for selecting candidate genes for further investigation. A total of 62 genes associated with nitrogen use efficiency in *Oryza sativa* were retrieved from Kumari et al. (2021) (Table 1) and subsequently blasted against the *Elaeis guineensis* genome.

Table 1. Global alignment of 62 genes related nitrogen use efficiency *of O. sativa* to *E. guineensis*

No	Genes symbol	Locus ID	Global alignment results to *E. guineensis*	Description of *E. guineensis* gene	Query Cover	Identity (%)	Acc. Length	Accession
1	*OsGOGAT2*	OS05g0555600	Q0DG35.2	glutamate synthase 1 [NADH], chloroplastic isoform X1 [*Elaeis guineensis*]	100	78.72	2185	XP_010913556.1
2	*bc6*	OS09g0422500	Q69P51.1	cellulose synthase A catalytic subunit 9 [UDP-forming] [*Elaeis guineensis*]	100	88.26	1048	XP_010905024.1
3	*OsGEN-L*	OS09g0521900	Q64MA3.1	flap endonuclease GEN-like 1 [*Elaeis guineensis*]	100	57.89	684	XP_010934428.2
4	*phyB*	OS03g0309200	Q10MG9.1	LOW QUALITY PROTEIN: phytochrome B [*Elaeis guineensis*]	100	79.18	1134	XP_010921452.1
5	*OsDWARF*	OS03g0602300	Q8GSQ1.1	cytochrome P450 85A1 [*Elaeis guineensis*]	100	72.55	465	XP_010923635.1
6	*OsSAMS1*	OS05g0135700	Q0DKY4.1	S-adenosylmethionine synthase [*Elaeis guineensis*]	100	94.44	396	XP_010921340.1
7	*OsMADS8*	OS09g0507200	Q9SAR1.1	MADS box transcription factor [*Elaeis guineensis*]	100	68.38	242	AAQ03224.1

No	Genes symbol	Locus ID	Global alignment results to *E. guineensis*	Description of *E. guineensis* gene	Query Cover	Identity (%)	Acc. Length	Accession
8	*OsSh1*	OS03g0650000	Q10FZ7.1	protein YABBY 2 [*Elaeis guineensis*]	100	63.3	215	XP_029116808.1
9	*nadh-gogat1*	OS01g0682001	BAS73718.1	glutamate synthase 1 [NADH], chloroplastic isoform X1 [*Elaeis guineensis*]	100	71.48	2185	XP_010913556.1
10	*Bc7(t)*	OS01g0750300	BAS74356.1	cellulose synthase A catalytic subunit 4 [UDP-forming] [*Elaeis guineensis*]	100	89.93	973	XP_010924731.1
11	*dgl1*	OS01g0683100	BAS73724.1	katanin p60 ATPase-containing subunit A1 isoform X1 [*Elaeis guineensis*]	100	84.84	519	XP_010925118.1
12	*OsACDR1*	OS03g0160100	BAS82406.1	serine/threonine-protein kinase EDR1 [*Elaeis guineensis*]	100	57.58	1017	XP_010917753.1
13	*GA2ox3*	OS01g0757200	Q8S0S6.1	gibberellin 2-beta-dioxygenase 3 [*Elaeis guineensis*]	100	65.15	328	XP_010919848.1
14	*OsSSI2*	OS01g0919900	Q8S059.1	stearoyl-[acyl-carrier-protein] 9-desaturase, chloroplastic-like [*Elaeis guineensis*]	100	81.61	393	XP_010927705.1
15	*Orysa;CycB1;1*	OS01g0805600	Q0JIF2.2	G2/mitotic-specific cyclin S13-7 isoform X1 [*Elaeis guineensis*]	100	65.49	446	XP_010931535.1
16	*OSH71*	OS05g0129700	Q7GDL5.1	homeobox protein knotted-1-like 1 [*Elaeis guineensis*]	100	66.98	318	NP_001290498.1
17	*OsLOX1*	OS03g0700700	Q53RB0.1	probable linoleate 9S-lipoxygenase 4 [*Elaeis guineensis*]	99	70.84	866	XP_010905215.1
18	*OsLOX2 (L-2)*	OS03g0738600	P29250.2	probable linoleate 9S-lipoxygenase 4 [*Elaeis guineensis*]	99	64.31	866	XP_010905215.1
19	*phyC*	OS03g0752100	Q10CQ8.1	phytochrome C [*Elaeis guineensis*]	99	75.82	1128	XP_010906221.1
20	*sgr*	OS09g0532000	Q652K1.1	protein STAY-GREEN homolog, chloroplastic [*Elaeis guineensis*]	99	63.64	268	XP_010907484.1
21	*OsZHD1*	OS09g0466400	Q6YXH5.1	zinc-finger homeodomain protein 2 [*Elaeis guineensis*]	99	61	281	XP_010939727.1

No	Genes symbol	Locus ID	Global alignment results to *E. guineensis*	Description of *E. guineensis* gene	Query Cover	Identity (%)	Acc. Length	Accession
22	*OsETT2*	OS01g0670800	Q0JKI9.1	auxin response factor 15 isoform X2 [*Elaeis guineensis*]	99	55.92	819	XP_029121009.1
23	*msp1*	OS01g0917500	Q8RZV7.1	leucine-rich repeat receptor protein kinase MSP1 [*Elaeis guineensis*]	99	63.83	1300	XP_010908331.1
24	*OsNAP*	OS03g0327800	Q8H7M1.1	NAC domain-containing protein 2 [*Elaeis guineensis*]	99	47.5	339	XP_010938117.1
25	*pdhk*	OS03g0370000	BAS84357.1	pyruvate dehydrogenase (acetyl-transferring) kinase, mitochondrial [*Elaeis guineensis*]	99	78.45	368	XP_010943866.1
26	*gamyb*	OS01g0812000	Q0JIC2.1	transcription factor GAMYB isoform X1 [*Elaeis guineensis*]	99	48.25	556	XP_029120531.1
27	*chl1*	OS03g0811100	Q6ATS0.1	magnesium-chelatase subunit ChlD, chloroplastic [*Elaeis guineensis*]	98	82.2	753	XP_010922222.1
28	*OsGH3.1*	OS01g0785400	Q8LQM5.1	probable indole-3-acetic acid-amido synthetase GH3.1 [*Elaeis guineensis*]	98	77.2	607	XP_010924006.1
29	*WLP1*	OS01g0749200	BAS74345.1	50S ribosomal protein L13, chloroplastic [*Elaeis guineensis*]	98	67.6	246	XP_010916493.1
30	*d61*	OS01g0718300	Q942F3.1	brassinosteroid LRR receptor kinase BRI1 [*Elaeis guineensis*]	98	67.18	1129	XP_010927763.1
31	*OsCKX4*	OS01g0940000	Q5JLP4.1	cytokinin dehydrogenase 4 [*Elaeis guineensis*]	98	70.89	527	XP_010938664.1
32	*OsDDM1a*	OS09g0442700	BAT08311.1	ATP-dependent DNA helicase DDM1 isoform X1 [*Elaeis guineensis*]	98	69.36	784	XP_019709878.1
33	*OsDREB1B*	OS09g0522000	Q3T5N4.1	dehydration-responsive element-binding protein 1C [*Elaeis guineensis*]	98	48.28	235	XP_010934429.1

No	Genes symbol	Locus ID	Global alignment results to *E. guineensis*	Description of *E. guineensis* gene	Query Cover	Identity (%)	Acc. Length	Accession
34	*shl2*	OS01g0527600	Q8LHH9.1	probable RNA-dependent RNA polymerase SHL2 [*Elaeis guineensis*]	98	64.3	1198	XP_010921974.1
35	*Gn1a*	OS01g0197700	Q4ADV8.1	cytokinin dehydrogenase 6 [*Elaeis guineensis*]	98	50.98	536	XP_010912967.1
36	*OsbZIP72*	OS09g0456200	BAT08433.1	bZIP transcription factor 46 isoform X1 [*Elaeis guineensis*]	97	50.59	403	XP_010943073.1
37	*glu1*	OS03g0329500	P0C1U4.1	endoglucanase 9 [*Elaeis guineensis*]	97	80.89	622	XP_010938102.1
38	*OsATG7*	OS01g0614900	BAS73152.1	ubiquitin-like modifier-activating enzyme atg7 [*Elaeis guineensis*]	97	49.86	718	XP_010924881.1
39	*RACK1A*	OS01g0686800	P49027.1	guanine nucleotide-binding protein subunit beta-like protein A [*Elaeis guineensis*]	97	82.77	323	XP_010923802.1
40	*cwa1/bc1*	OS03g0416200	Q10JL1.1	COBRA-like protein 4 [*Elaeis guineensis*]	96	72.54	466	XP_010936445.1
41	*GH3-2*	OS01g0764800	P0C0M2.1	probable indole-3-acetic acid-amido synthetase GH3.8 [*Elaeis guineensis*]	96	77.33	594	XP_010939642.1
42	*OsOAT*	OS03g0643300	Q10G56.1	ornithine aminotransferase, mitochondrial [*Elaeis guineensis*]	96	81.72	474	XP_010940988.1
43	*Osppc4*	OS01g0208700	NP_001391814.1	SCAR-like protein 2 [*Elaeis guineensis*]	96	76.38	2192	XP_010925637.2
44	*OsDREB1A*	OS09g0522200	Q64MA1.1	dehydration-responsive element-binding protein 1C [*Elaeis guineensis*]	95	47.06	236	XP_010940896.1
45	*chl9*	OS03g0563300	A0A6I9QWL2	magnesium-chelatase subunit ChlI, chloroplastic [*Elaeis guineensis*]	95	81.77	427	XP_010915593.1
46	*se13*	OS01g0949400	BAS76225.1	phytochromobilin:ferredoxin oxidoreductase, chloroplastic isoform X2 [*Elaeis guineensis*]	95	68.07	291	XP_010924238.1

No	Genes symbol	Locus ID	Global alignment results to *E. guineensis*	Description of *E. guineensis* gene	Query Cover	Identity (%)	Acc. Length	Accession
47	*OsYUCCA1*	OS01g0645400	A0A0P0V5U9.1	indole-3-pyruvate monooxygenase YUCCA1 isoform X1 [*Elaeis guineensis*]	95	68.48	403	XP_010923752.1
48	*OsRRMh*	OS09g0516300	BAT08962.1	flowering time control protein FPA [*Elaeis guineensis*]	94	42.18	984	XP_010908978.1
49	*sd1*	OS01g0883800	Q0JH50.1	gibberellin 20 oxidase 2 [*Elaeis guineensis*]	94	62.53	377	XP_010911046.1
50	*eg1*	OS01g0900400	Q8S1D9.1	phospholipase A1-Ialpha2, chloroplastic [*Elaeis guineensis*]	94	57.65	439	XP_010912884.1
51	*RGB1*	OS03g0669100	BAS85668.1	deoxyuridine 5'-triphosphate nucleotidohydrolase [*Elaeis guineensis*]	90	66.86	230	XP_019709548.1
52	*OsMT2b*	OS05g0111300	A3AZ88.1	metallothionein-like protein 2A [*Elaeis guineensis*]	89	47.37	77	XP_010922336.1
53	*OsRZFP34*	OS01g0719100	Q5JL96.1	probable E3 ubiquitin-protein ligase RZFP34 [*Elaeis guineensis*]	88	76.03	308	XP_010917209.1
54	*OsPIL1*	OS03g0782500	Q10CH5.1	transcription factor PHYTOCHROME INTERACTING FACTOR-LIKE 13 isoform X8 [*Elaeis guineensis*]	87	45.43	544	XP_029116710.1
55	*pla3/gp*	OS03g0790600	Q852M4.2	probable glutamate carboxypeptidase VP8 isoform X1 [*Elaeis guineensis*]	87	66.51	707	XP_010908056.1
56	*BC15/OsCTL1*	OS09g0494200	BAT08769.1	chitinase-like protein 1 [*Elaeis guineensis*]	86	78.29	300	XP_010927492.1
57	*OsPAO*	OS03g0146400	Q0DV66.1	pheophorbide a oxygenase, chloroplastic [*Elaeis guineensis*]	85	83.85	551	XP_010918717.1
58	*log*	OS01g0588900	Q5ZC82.1	cytokinin riboside 5'-monophosphate phosphoribohydrolase LOG7 [*Elaeis guineensis*]	82	80.81	240	XP_010925070.1
59	*OsMADS51*	OS01g0922800	Q9XJ61.1	MADS-box transcription factor 51	82	53.15	203	XP_010926839.1

No	Genes symbol	Locus ID	Global alignment results to *E. guineensis*	Description of *E. guineensis* gene	Query Cover	Identity (%)	Acc. Length	Accession
				isoform X2 [*Elaeis guineensis*]				
60	*OsIPT7*	OS05g0551700	BAS95219.1	adenylate isopentenyltransferase [*Elaeis guineensis*]	81	53.9	357	XP_010927008.1
61	*OsHO2*	OS03g0395000	Q10K62.1	probable inactive heme oxygenase 2, chloroplastic [*Elaeis guineensis*]	77	55.73	296	XP_010916650.1
62	*DEP1*	OS09g0441900	Q67UU9.1	guanine nucleotide-binding protein subunit gamma 3 [*Elaeis guineensis*]	47	47.43	195	XP_010937332.1

After performing a global alignment, we filtered out genes with a query cover and similarity greater than 80% to improve accuracy in identifying *E. guineensis* genes. This process eliminated 50 candidate genes, leaving 12 genes related to nitrogen use efficiency, including *bc6*, *OsSAMS1*, *Bc7(t)*, *dgl1*, *OsSSI2*, *chl1*, *glu1*, *RACK1A*, *OsOAT*, *chl9*, *OsPAO*, and *log* (Table 2). While we prioritized genes with high protein similarity, it is possible that other potential marker genes could be missed due to lower similarity percentages. This is because protein similarity can be influenced by evolutionary differences (Theobald and Wuttke 2005). In this study, *O. sativa* and *E. guineensis* are hypothesized to have diverged from different ancestors, which may contribute to variations in protein sequence similarity. Here, we successfully extracted twelve genes from the global alignment, which we hypothesize to be important regulators of nitrogen use efficiency. These twelve genes were then subjected to PPI analysis.

Table 2. Twelve genes-related-nitrogen use efficiency after filtering from query cover and similarity >80% parameters

No	Genes symbol	Locus ID	Global alignment results to *E. guineensis*	Description of *E. guineensis* gene	Query Cover	Identity (%)	Acc. Len	Accession
1	*bc6*	OS09g0422500	Q69P51.1	cellulose synthase A catalytic subunit 9 [UDP-forming] [*Elaeis guineensis*]	100	88.26	1048	XP_010905024.1
2	*OsSAMS1*	OS05g0135700	Q0DKY4.1	S-adenosylmethionine synthase [*Elaeis guineensis*]	100	94.44	396	XP_010921340.1
3	*Bc7(t)*	OS01g0750300	BAS74356.1	cellulose synthase A catalytic subunit 4 [UDP-forming] [*Elaeis guineensis*]	100	89.93	973	XP_010924731.1
4	*dgl1*	OS01g0683100	BAS73724.1	katanin p60 ATPase-containing subunit A1 isoform X1 [*Elaeis guineensis*]	100	84.84	519	XP_010925118.1

No	Genes symbol	Locus ID	Global alignment results to *E. guineensis*	Description of *E. guineensis* gene	Query Cover	Identity (%)	Acc. Len	Accession
5	*OsSSI2*	OS01g0919900	Q8S059.1	stearoyl-[acyl-carrier-protein] 9-desaturase, chloroplastic-like [*Elaeis guineensis*]	100	81.61	393	XP_010927705.1
6	*chl1*	OS03g0811100	Q6ATS0.1	magnesium-chelatase subunit ChlD, chloroplastic [*Elaeis guineensis*]	98	82.2	753	XP_010922222.1
7	*glu1*	OS03g0329500	P0C1U4.1	endoglucanase 9 [*Elaeis guineensis*]	97	80.89	622	XP_010938102.1
8	*RACK1A*	OS01g0686800	P49027.1	guanine nucleotide-binding protein subunit beta-like protein A [*Elaeis guineensis*]	97	82.77	323	XP_010923802.1
9	*OsOAT*	OS03g0643300	Q10G56.1	ornithine aminotransferase, mitochondrial [*Elaeis guineensis*]	96	81.72	474	XP_010940988.1
10	*chl9*	OS03g0563300	A0A6I9QWL2	magnesium-chelatase subunit ChlI, chloroplastic [*Elaeis guineensis*]	95	81.77	427	XP_010915593.1
11	*OsPAO*	OS03g0146400	Q0DV66.1	pheophorbide a oxygenase, chloroplastic [*Elaeis guineensis*]	85	83.85	551	XP_010918717.1
12	*log*	OS01g0588900	Q5ZC82.1	cytokinin riboside 5'-monophosphate phosphoribohydrolase LOG7 [*Elaeis guineensis*]	82	80.81	240	XP_010925070.1

Protein-protein interaction networks analysis

Twelve genes related to nitrogen use efficiency from *Oryza sativa* were analyzed using the STRING database, resulting in the formation of two distinct network clusters. *Elaeis guineensis* was not used as the reference organism, as its genome is not available in the STRING database. The predicted interactions were categorized into gene fusions (represented by red lines), neighbourhood associations (green lines), and co-occurrence relationships (blue lines) (Figure 2).

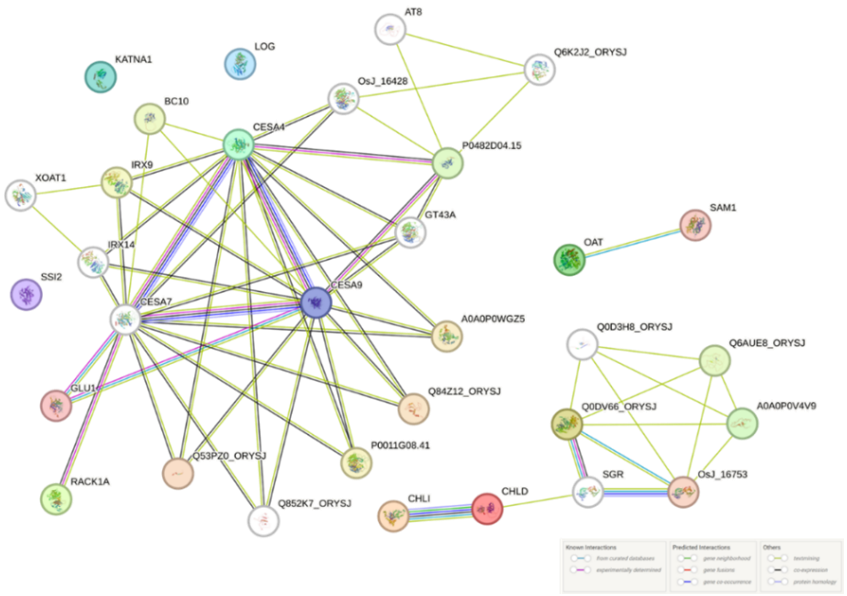

Figure 2. Protein-protein interaction of twelve genes related nitrogen use efficiency from *O. sativa*

To assess gene functionality, STRING-db automatically generates gene ontology (GO) analysis based on the input genes. The identified terms were categorized into two groups of functionally similar genes, with a similarity value greater than 0.8 (Figure 3). The most significantly enriched biological processes (BP) were associated with plant-type secondary cell walls and cellular metabolic processes, with enrichment scores ranging from 5.5 to 7.5 (Figure 3A). The relationship between plant secondary cell walls and nitrogen use efficiency is complex, influenced by various factors, including nitrogen availability, cell wall composition, and genetic regulation. A study on *Polygonum cuspidatum* demonstrated that nitrogen allocation to cell walls can reduce photosynthetic nitrogen-use efficiency. Specifically, plants with higher nitrogen allocation to cell walls exhibited reduced photosynthetic capacity, suggesting a trade-off between structural nitrogen investment and photosynthetic efficiency (Onoda et al. 2004).

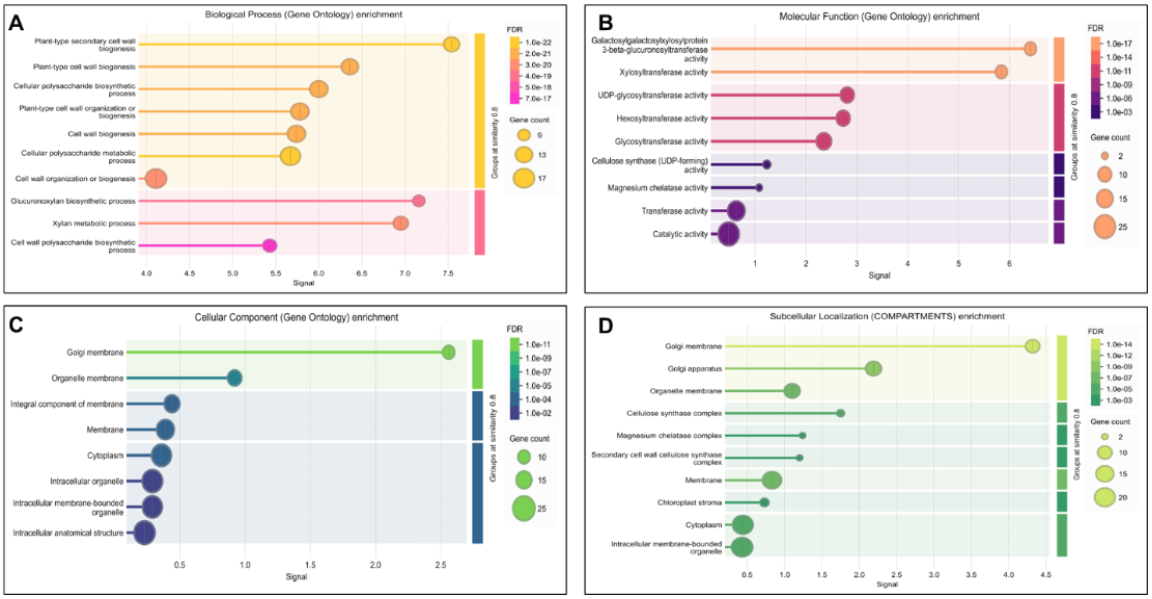

Figure 2. Functional enrichment of biological process (BP) (A), molecular function (MF) (B), cellular component (CC) (C), and subcellular location (SC) (D)

Additionally, research on *Eucalyptus* species revealed that nitrogen fertilization levels affect xylem gene expression and secondary cell wall lignification. Excessive nitrogen fertilization led to lower lignin content and altered lignin composition in the xylem, indicating that nitrogen availability can influence the structural properties of secondary cell walls (Camargo et al. 2014). Similarly, studies on *Sorghum* seedlings showed that nitrogen deficiency led to changes in cell wall composition, including modifications in lignin content and structure. These findings suggest that nitrogen availability plays a crucial role in the biosynthesis and remodelling of secondary cell walls, which may impact nitrogen use efficiency (Rivai et al. 2021).

Furthermore, a comparative analysis of C3 and C4 plants examined the effects of type 1 and type 2 cell wall architectures on nitrogen utilization. The study found that C4 grasses, which possess type 2 cell walls, exhibited higher nitrogen use efficiency, particularly under nitrogen-deficient conditions. This suggests that cell wall architecture may contribute to optimizing nitrogen utilization (Bossoni et al. 2022).

Moreover, molecular function (MF) enrichment analysis indicated that Galactosylgalactosylxylosylprotein 3-beta-glucuronosyltransferase exhibited the highest activity, with a signal strength of approximately 6.5, followed by Xylosyltransferase activity, which ranked second with a signal just below 6 (Figure 3B). Meanwhile, cellular component (CC) and subcellular compartment (SC) enrichment results identified the Golgi membrane as the primary location of these enriched genes (Figure 3C-D).

Galactosylgalactosylxylosylprotein 3-beta-glucuronosyltransferase, also known as beta-1,3-glucuronyltransferase 3 and encoded by the B3GAT3 gene, is an enzyme essential for the biosynthesis of glycosaminoglycans (GAGs), such as heparan sulfate and chondroitin sulfate, which are crucial components of the extracellular matrix in animal tissues. However, in plants, glycosyltransferases from the GT47 family play significant roles in cell wall biosynthesis. Some members of this family function as β-glucuronyltransferases, contributing to the synthesis of pectic polysaccharides. For instance, the GlcAT14 family of glycosyltransferases in *Arabidopsis thaliana* is responsible for adding glucuronic acid residues to arabinogalactan proteins (AGPs), which are essential components of the plant cell wall (Zhong and Ye 2003).

Similarly, xylosyltransferases catalyze the transfer of xylose residues from UDP-xylose to specific acceptor molecules, playing a vital role in the biosynthesis and modification of various plant polysaccharides and glycoproteins. One type, xylogalacturonan beta-1,3-xylosyltransferase, transfers a xylosyl residue from UDP-D-xylose to a D-galactose residue in xylogalacturonan, forming a β-1,3-D-xylosyl-D-galactose linkage (Jensen et al. 2008). Another type, xyloglucan 6-xylosyltransferase, catalyzes the transfer of an α-D-xylosyl residue from UDP-D-xylose to a glucose residue in xyloglucan, forming an α-1,6-D-xylosyl-D-glucose bond. This reaction is crucial for the proper assembly of xyloglucan, a major hemicellulosic polysaccharide in plant cell walls (Faik et al. 2000).

Pathway enrichment analysis was also conducted using KEGG enrichment (Figure 4). The highest enrichment signal was associated with porphyrin and chlorophyll metabolism, with a value exceeding 1.4. This pathway includes the genes *Q0DV66_ORYSJ, OsJ_16753, CHLI, SGR*, and *CHLD*.

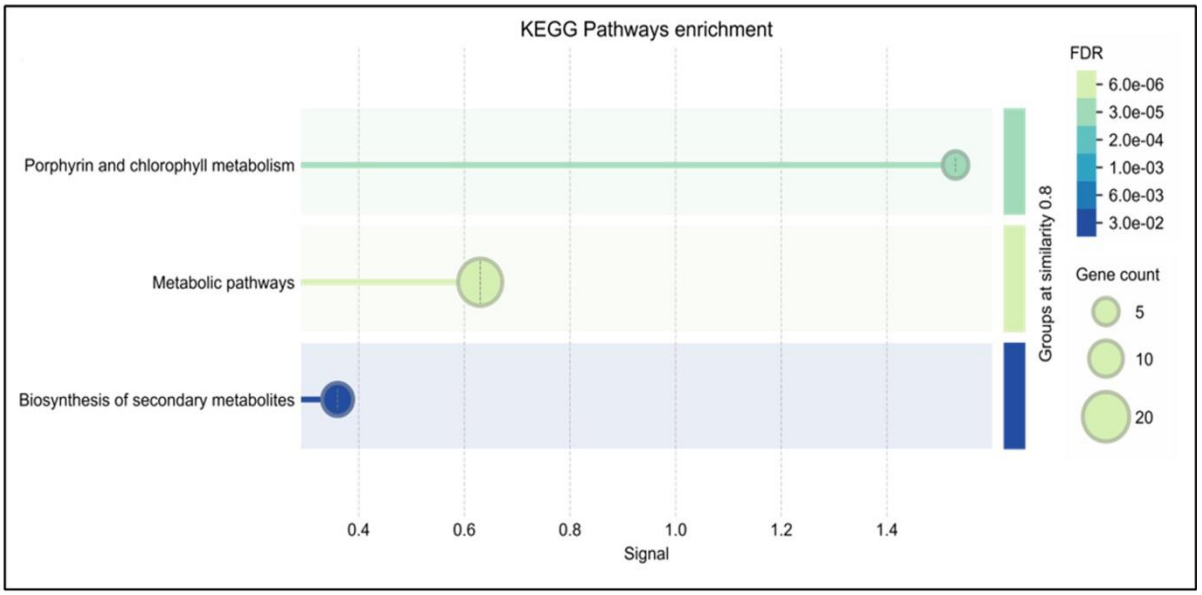

Figure 4. Functional enrichment of KEGG pathway

Porphyrin and chlorophyll metabolism are closely related to nitrogen use efficiency in plants, as nitrogen is a key component of chlorophyll molecules, which are essential for photosynthesis. Consequently, nitrogen availability directly affects chlorophyll synthesis, influencing photosynthetic capacity and overall plant growth. In wheat, nitrogen plays a crucial role in plant nutrition by supporting protein and nucleic acid synthesis. Different cultivars exhibit varying responses to nitrogen availability, and total nitrogen content serves as an indicator of root activity and nutrient translocation. Moreover, nitrogen promotes leaf growth, enhancing photosynthetic efficiency. Since photosynthetic proteins constitute a significant portion of leaf nitrogen, chlorophyll levels are strongly correlated with nitrogen content (Bojović and Marković 2009). Thus, efficient nitrogen utilization is critical for optimizing plant growth and productivity.

The second most enriched pathway was general metabolic pathways, with an enrichment signal of 0.6. This category includes the genes *OsJ_16428, GLU1, SAM1, OAT, Q53PZ0_ORYSJ, CHLI, CESA4, P0011G08.41, IRX14, CESA9, CHLD, Q6K2J2_ORYSJ, IRX9, GT43A, Q84Z12_ORYSJ, Q852K7_ORYSJ, SSI2,* and *P0482D04.15.* The final enriched pathway was the biosynthesis of secondary metabolites, with an enrichment signal of less than 0.4. This pathway involves the genes *SAM1, Q0DV66_ORYSJ, OsJ_16753, OAT, CHLI, SGR, CHLD,* and *Q6K2J2_ORYSJ.*

Network analysis using Cytoscape

To enhance the analysis, the TSV file from STRING-db was imported into Cytoscape to examine network interactions. In Cytoscape, node network analysis was configured based on degree values, while edge analysis was determined by betweenness values. Additionally, node and edge colors were scaled from the minimum value (magenta) to the maximum value (dark green) (Figure 5).

Figure 5. PPI network of 12 genes related to nitrogen use efficiency from *O. sativa*. Nodes with high degree are illustrated by bigger size and darker green colors. Edge with high betweeness depicts by bolder line and darker green colors

Degree centrality represents the number of connections a node has within a network. In protein-protein interaction (PPI) networks, nodes with a higher degree are considered hubs, typically occupying central positions in the network (Barabási et al. 2011). Meanwhile, betweenness centrality measures how frequently a node appears on the shortest paths between other nodes. Nodes with high betweenness, known as bottlenecks, regulate the flow of information within the network (Zhang 2009).

In this study, the network revealed three key genes with the highest degree values: *CESA4*, *CESA7*, and *CESA9*, each displaying a directed network of 13 to 14 connected genes. Specifically, *CESA4* exhibits directed connections to *OsJ_16428*, *Q53PZ0_ORYSJ*, *P0482D04.15*, *P0011G08.41*, *Q84Z12_ORYSJ*, *Q852K7_ORYSJ*, *GT43A*, *IRX14*, *IRX9*, *CESA7*, and *CESA9*. Meanwhile, *CESA7* directly targets *OsJ_16428*, *GLU1*, *RACK1A*, *Q53PZ0_ORYSJ*, *P0011G08.41*, *IRX14*, *CESA9*, *IRX9*, *GT43A*, *Q84Z12_ORYSJ*, and *Q852K7_ORYSJ*. Lastly, *CESA9* directs connections to *GLU1*, *Q53PZ0_ORYSJ*, *P0011G08.41*, *IRX14*, *P0482D04.15*, *Q84Z12_ORYSJ*, *Q852K7_ORYSJ*, *GT43A*, and *IRX9*.

After analyzing the PPI network, cellulose synthase (CESA) was identified as the most significant gene in the system for nitrogen use efficiency-related genes, based on both degree and betweenness values. Subsequently, we examined the structural similarity between CESA4 and CESA9 in *O. sativa* and *E. guineensis*. The 3D models were evaluated using a Ramachandran plot, both models were then superimposed, and their root mean square deviation (RMSD) values were evaluated to compare structural differences.

Ramachandran plot analysis of four modelled protein: OsCESA4, EgCESA4, OsCESA9, EgCESA9 exhibit favoured region more than 90% (Figure 6). A high-resolution input structure is expected to achieve a quality score exceeding 95%. Protein structures with a resolution between 2 and 3 Å generally exhibit a quality score above 90% (Agnihotry et al., 2022).

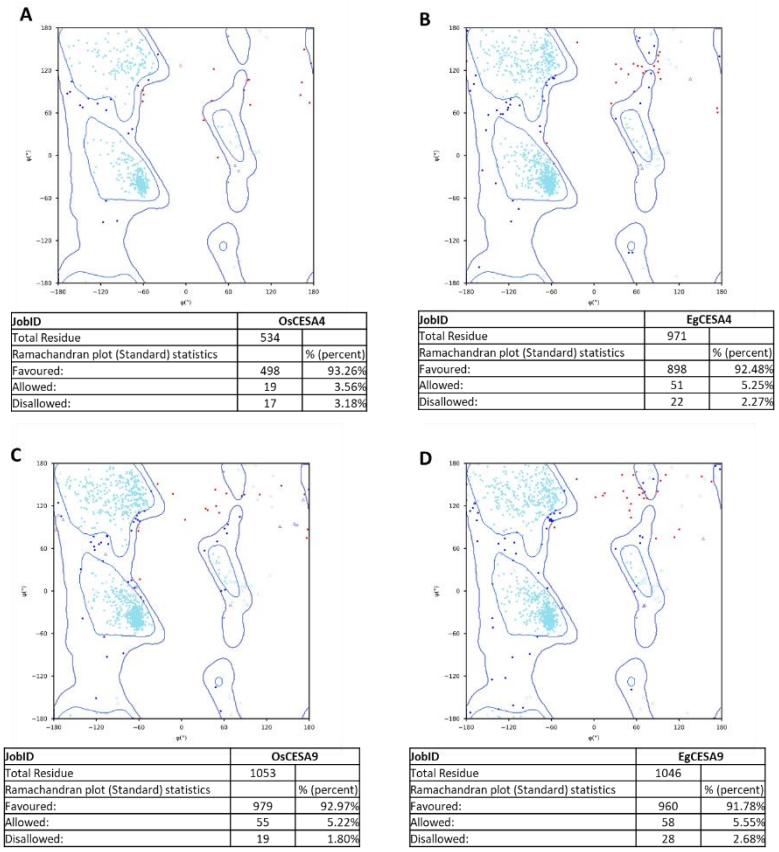

JobID	OsCESA4	
Total Residue	534	
Ramachandran plot (Standard) statistics		% (percent)
Favoured:	498	93.26%
Allowed:	19	3.56%
Disallowed:	17	3.18%

JobID	EgCESA4	
Total Residue	971	
Ramachandran plot (Standard) statistics		% (percent)
Favoured:	898	92.48%
Allowed:	51	5.25%
Disallowed:	22	2.27%

JobID	OsCESA9	
Total Residue	1053	
Ramachandran plot (Standard) statistics		% (percent)
Favoured:	979	92.97%
Allowed:	55	5.22%
Disallowed:	19	1.80%

JobID	EgCESA9	
Total Residue	1046	
Ramachandran plot (Standard) statistics		% (percent)
Favoured:	960	91.78%
Allowed:	58	5.55%
Disallowed:	28	2.68%

Figure 6. Ramachandran plot from Alphafold software of (A) OsCESA4, (B) EgCESA4, (C) OsCESA9, (D) EgCESA9 structure

The RMSD analysis revealed that CESA4 in *O. sativa* and *E. guineensis* had a lower RMSD value of 0.338 Å, whereas CESA9 exhibited a slightly higher RMSD value of 0.396 Å (Figure 7). RMSD is a commonly used metric for assessing structural similarity between proteins. Typically, an RMSD of ≤2 Å indicates high structural similarity, while values ranging from 2 to 5 Å suggest moderate similarity. Higher RMSD values indicate greater structural deviations (Kufareva and Abagyan 2012). Based on these results, the structures of CESA4 and CESA9 in *O. sativa* and *E. guineensis* exhibit a high degree of similarity.

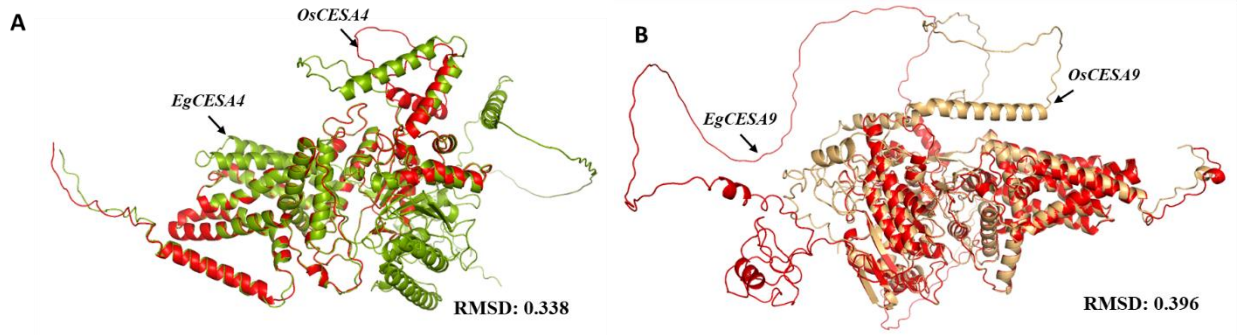

Figure 7. Superpose of 3D structure protein (a) CESA4 in *E. guineensis* (green, cartoon) and *O. sativa* (red, cartoon), (b) CESA9 in *E. guineensis* (red, cartoon) and *O. sativa* (wheat, cartoon)

The *CESA* protein in *O. sativa* shares similarities with the cellulose synthase A catalytic subunit [UDP-forming] in *E. guineensis*. *CESA* proteins play a crucial role in cellulose biosynthesis in *E. guineensis* (African oil palm), contributing to cell wall formation and plant structural integrity. A study identified six genes related to *CESA* and cellulose synthase-like D (*CSL*), which are involved in cell wall modification in *E. guineensis*. Notably, the transcription factors *EgJUB1* and *EgERF113* were highlighted as potential regulators of these genes, suggesting their significant role in modulating cellulose biosynthesis (Sakeh et al. 2021).

The relationship between *CESA* proteins and nitrogen use efficiency in plants is an emerging area of research. While direct studies on *CESA*'s role in nitrogen use efficiency remain limited, existing research provides insights into potential connections: (a) Impact of nitrogen on cellulose biosynthesis: Nitrogen availability influences cellulose production in plants. A study on rice (*O. sativa*) found that overexpression of the transcription factor *OsMYB305* suppressed cellulose biosynthesis under low-nitrogen conditions. This suppression redirected carbohydrates toward nitrate uptake and assimilation, enhancing plant growth and nitrogen use efficiency (Wang et al. 2020), (b) Nutrient deficiencies and *CESA* expression. The availability of nutrients, including nitrogen, can regulate *CESA* gene expression. In soybeans (*Glycine max*), nitrogen deficiency led to adjustments in nitrogen uptake and utilization efficiency, potentially affecting cellulose synthesis pathways (Nezamivand-Chegini et al. 2022).

These findings suggest that nitrogen availability is able to influence cellulose biosynthesis by modulating cellulose synthase (CESA) activity, thereby impacting plant growth and nitrogen use efficiency. However, to establish CESA as a molecular marker for nitrogen-use efficiency-related genes, further research is necessary to elucidate the direct mechanisms linking CESA proteins to nitrogen-use efficiency.

CONCLUSION

This study identified 12 nitrogen use efficiency-related genes in *Elaeis guineensis* through global alignment with *Oryza sativa*. Protein-protein interaction analysis highlighted *CESA* genes as key regulators. Structural modeling and RMSD analysis confirmed their similarity between species. Pathway enrichment linked nitrogen availability to cell wall biosynthesis and metabolic regulation. These findings suggest a potential role of *CESA* genes in optimizing nitrogen use efficiency, offering valuable insights for oil palm breeding through molecular marker-assisted selection. However, evaluation through in vitro experiment needed to be done to validate the CESA's protein contribution in nitrogen-use efficiency.

STATEMENT OF INTEREST

The authors declare no financial, professional, or personal conflicts of interest that could have influenced the conduct or presentation of this study.

ACKNOWLEDGMENT

The authors would like to thank the Indonesian Oil Palm Research Institute - PT Riset Perkebunan Nusantara for supporting this research. This study was funded by *Badan Pengelola Dana Perkebunan Kelapa Sawit* (BPDPKS).

REFERENCES

Agnihotry S, Rajesh KP, Dev BS, Apoorv T, Imran H (2022) Chapter 11 - Protein structure prediction. Academic Press. doi.org/10.1016/B978-0-323-89775-4.00023-7.

Barabási A-L, Gulbahce N, Loscalzo J (2011) Network medicine: a network-based approach to human disease. Nat Rev Genet 12:56–68. doi: 10.1038/nrg2918

Bojović B, Marković A (2009) Correlation between nitrogen and chlorophyll content in wheat (*Triticum aestivum* L.). Kragujev J Sci 31:69–74

Bossoni GEB, Stata M, Almeida AM, Constantin RP, Ferrarese-Filho O, Sage RF, dos Santos WD (2022) Cell wall nitrogen use efficiency: Assessing the impact of type 1 and type 2 cell wall

architectures on the nitrogen economy in C3 and C4 plants

Camargo ELO, Nascimento LC, Soler M, Salazar MM, Lepikson-Neto J, Marques WL, Alves A, Teixeira PJPL, Mieczkowski P, Carazzolle MF, Martinez Y, Deckmann AC, Rodrigues JC, Grima-Pettenati J, Pereira GAG (2014) Contrasting nitrogen fertilization treatments impact xylem gene expression and secondary cell wall lignification in *Eucalyptus*. BMC Plant Biol 14:256. doi:10.1186/s12870-014-0256-9.

Corley RH V, Tinker PB (2016) The Oil Palm, Fifth Edition. Wiley Blackwell, Chichester

Doncheva NT, Morris JH, Holze H, Kirsch R, Nastou KC, Cuesta-Astroz Y, Rattei T, Szklarczyk D, von Mering C, Jensen LJ (2002) Cytoscape stringApp 2.0: Analysis and Visualization of Heterogeneous Biological Networks. J Proteome Res 22(2):637-646. doi: 10.1021/acs.jproteome.2c00651.

Faik A, Bar-Peled M, DeRocher AE, Zeng W, Perrin RM, Wilkerson C, Raikhel N V., Keegstra K (2000) Biochemical characterization and molecular cloning of an α-1,2-fucosyltransferase that catalyzes the last step of cell wall xyloglucan biosynthesis in pea. J Biol Chem 275:15082–15089. doi: 0.1074/jbc.M000677200

Jensen JK, Sørensen SO, Harholt J, Geshi N, Sakuragi Y, Møller I, Zandleven J, Bernal AJ, Jensen NB, Sørensen C, Pauly M, Beldman G, Willats WGT, Scheller HV (2008) Identification of a xylogalacturonan xylosyltransferase involved in pectin biosynthesis in *Arabidopsis*. Plant Cell 20:1289–1302. doi: 10.1105/TPC.107.050906

Jumper J, Evans R, Pritzel A, Green T, Figurnov M, Ronneberger O, Tunyasuvunakool K, Bates R, Žídek A, Potapenko A, Bridgland A, Meyer C, Kohl SAA, Ballard AJ, Cowie A, Romera-Paredes B, Nikolov S, Jain R, Adler J, Back T, Petersen S, Reiman D, Clancy E, Zielinski M, Steinegger M, Pacholska M, Berghammer T, Bodenstein S, Silver D, Vinyals O, Senior AW, Kavukcuoglu K, Kohli P, Hassabis D (2021) Highly accurate protein structure prediction with AlphaFold. Nature 596:583–589. doi: 10.1038/s41586-021-03819-2

Kufareva I, Abagyan R (2012) Methods of protein structure comparison. Methods Mol Biol 857:231–257. doi: 10.1007/978-1-61779-588-6_10

Kumari S, Sharma N, Raghuram N (2021) Meta-analysis of yield-related and N-responsive genes reveals chromosomal hotspots, key processes and candidate genes for nitrogen-use efficiency in rice. Front Plant Sci 12. doi: 10.3389/fpls.2021.627955

Kusin FM, Akhir NIM, Mahamat-Yusuff F, Auang M (2015) The impact of nitrogen fertilizer use on greenhouse gas emissions in an oil palm plantation associated with land use change. Atmósfera 28:243–250. doi: 10.20937/ATM.2015.28.04.03

Lau BYC, Othman A, Ramli US (2018) Application of proteomics technologies in oil palm research. Protein J 37:473–499. doi: 10.1007/s10930-018-9802-x

Lema, M (2018) Marker Assisted Selection in Comparison to Conventional Plant Breeding: Review Article. J Agric Sci Technol 14(2): 555914.

Maryanto SD, Tanjung ZA, Roberdi R, Sudania W, Made, Pujianto P, Hairinsyah H, Utomo C, Liwang T (2021) Involvement of purple acid phosphatase gene into nitrogen uptake of oil palm (*Elaeis guineensis*). Biodiversitas J Biol Divers 22. doi: 10.13057/biodiv/d220340

Nezamivand-Chegini M, Metzger S, Moghadam A, Tahmasebi A, Koprivova A, Eshghi S, Mohammadi-Dehchesmeh M, Kopriva S, Niazi A, Ebrahimie E (2022) Nitrogen and phosphorus deficiencies alter primary and secondary metabolites of soybean roots. ioRxiv preprint. doi: http://dx.doi.org/10.1101/2022.03.14.484309

Onoda Y, Hikosaka K, Hirose T (2004) Allocation of nitrogen to cell walls decreases photosynthetic nitrogen-use efficiency. Funct Ecol 18:419–425. doi: 10.1111/j.0269-8463.2004.00847.x

Rivai RR, Miyamoto T, Awano T, Takada R, Tobimatsu Y, Umezawa T, Kobayashi M (2021) Nitrogen deficiency results in changes to cell wall composition of sorghum seedlings. Sci Rep 11:23309. doi: 10.1038/s41598-021-02570-y

Ruiz-Romero R, De la Peña M, Ayala-Díaz I, Montoya C, Romero HM (2024) Genotype and nitrogen source influence drought stress response in oil palm seedlings. Agronomy 14:2082. doi: 10.3390/AGRONOMY14092082

Sakeh NM, Abdullah SNA, Bahari MNA, Azzeme AM, Shaharuddin NA, Idris AS (2021) EgJUB1 and EgERF113 transcription factors as potential master regulators of defense response in Elaeis guineensis against the hemibiotrophic *Ganoderma boninense*. BMC Plant Biol 21:59. doi: 10.1186/s12870-020-02812-7

Sun H, Qian Q, Wu K, Luo J, Wang S, Zhang C, Ma Y, Liu Q, Huang X, Yuan Q, Han R, Zhao M, Dong G, Guo L, Zhu X, Gou Z, Wang W, Wu Y, Lin H, Fu X (2014) Heterotrimeric G proteins regulate nitrogen-use efficiency in rice. Nat Genet 46:652–656. doi: 10.1038/ng.2958

Szklarczyk D, Gable AL, Nastou KC, Lyon D, Kirsch R, Pyysalo S, Doncheva NT, Legeay M, Fang T, Bork P, Jensen LJ, von Mering C (2021) The STRING database in 2021: customizable protein–protein networks, and functional characterization of user-uploaded gene/measurement sets. Nucleic Acids Res 49:D605–D612. doi: 10.1093/nar/gkaa1074

Theobald DL, Wuttke DS (2005) Divergent evolution within protein superfolds inferred from profile-based phylogenetics. J Mol Biol 354:722–737. doi: 10.1016/j.jmb.2005.08.071

The PyMOL Molecular Graphics System, Version 2.5.4, Schrödinger, LLC

Wang D, Xu T, Yin Z, Wu W, Geng H, Li L, Yang M, Cai H, Lian X (2020) Overexpression of OsMYB305 in rice enhances the nitrogen uptake under low-nitrogen condition. Front Plant Sci 11. doi: 10.3389/fpls.2020.00369

Wei Q, Wei Q, Xu J, Liu Y, Wang D, Chen S, Qian W, He M, Chen P, Zhou X, Qi Z (2024) Nitrogen losses from soil as affected by water and fertilizer management under drip irrigation: Development, hotspots and future perspectives. Agric Water Manag 296:108791. doi: 10.1016/j.agwat.2024.108791

Zhang A (2009) Protein Interaction Networks: Computational Analysis. Cambridge University Press, Buffalo

Zhong R, Ye Z-H (2003) Unraveling the functions of glycosyltransferase family 47 in plants. Trends Plant Sci 8:565–568. doi: 10.1016/j.tplants.2003.10.003